



Pair Approximation for Lattice Models with Multiple Interaction Scales

STEPHEN P. ELLNER*†‡

**Department of Ecology and Evolutionary Biology, Cornell University, E145 Corson Hall, Ithaca, NY 14853-2701, U.S.A.* †*Center for Applied Mathematics, Cornell University, E145 Corson Hall, Ithaca, NY 14853-2701, U.S.A.*

(Received on 1 December 2000, Accepted in revised form on 23 March 2001)

Pair approximation has frequently proved effective for deriving qualitative information about lattice-based stochastic spatial models for population, epidemic and evolutionary dynamics. Pair approximation is a moment closure method in which the mean-field description is supplemented by approximate equations for the frequencies of neighbor-site pairs of each possible type. A limitation of pair approximation relative to moment closure for continuous space models is that all modes of interaction between individuals (e.g., dispersal of offspring, competition, or disease transmission) are assumed to operate over a single spatial scale determined by the size of the interaction neighborhood. In this paper I present a multiscale pair approximation which allows different sized neighborhoods for each type of interaction. To illustrate and test the approximation I consider a spatial single-species logistic model in which offspring are dispersed across a *birth neighborhood* and established individuals have a death rate depending on the population density in a *competition neighborhood*, with one of these neighborhoods nested inside the other. Analysis of the steady-state equations yields several qualitative predictions that are confirmed by simulations of the model, and numerical solutions of the dynamic equations provide a close approximation to the transient behavior of the stochastic model on a large lattice. The multiscale pair approximation thus provides a useful intermediate between the standard pair approximation for a single interaction neighborhood, and a complete set of moment equations for more spatially detailed models.

© 2001 Academic Press

1. Introduction

Stochastic spatial models, which explicitly represent discrete individuals and their locations in space (Durrett, 1999) have become increasingly important in theoretical ecology over the last decade (e.g., Dieckmann *et al.*, 2000; Tilman & Kareiva, 1997). It is now widely appreciated that spatial patterns resulting from the small-scale randomness of individual births, deaths and movement can have significant impacts on

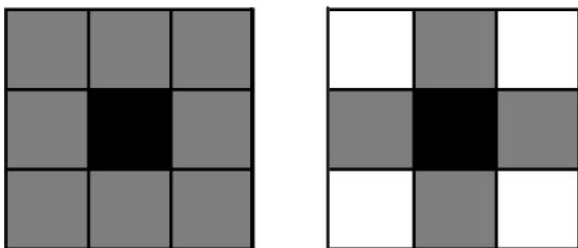
larger-scale aspects of the dynamics such as species coexistence, persistence of a disease, and spatiotemporal patterns such as patchiness, waves, spirals or cycles. Consequently, according to Law *et al.* (2000) “this is the age of the individual-based, spatially explicit, computer-based model”. These models are especially appealing to experimental ecologists because they can be derived, parameterized, and simulated by translating directly into computer code the assumed rules at the level of an individual, without any need for advanced mathematics (Wissel, 2000).

A disadvantage of stochastic spatial models is their analytic intractability relative to

‡ Cornell University, Department of Ecology and Evolutionary Biology, E145 Corson Hall, Ithaca, NY 14853-2701, U.S.A. E-mail: spe2@cornell.edu

metapopulation or reaction–diffusion models for spatial dynamics. Although more is known each year (Durrett, 1999), rigorous analytic results are typically limited to qualitative information such as existence of stationary distributions and persistence vs. extinction, or to limiting cases such as long-range interactions or rapid mixing (Durrett & Levin, 2000; Neuhauser, 1998). More detailed information can only be derived by simulation or through approximations. As Sato *et al.* (1994) note, a tractable approximation can make it possible to identify aspects of model behavior that would have been difficult to obtain from simulations alone. Interesting predictions from the approximation can then be verified by simulations in the appropriate parts of parameter space.

The pair approximation (PA), introduced for ecological models by Matsuda *et al.* (1992), has emerged as a useful approximation method for lattice models. Lattice models (also called stochastic cellular automata or “artificial ecologies”) represent space as a discrete lattice of sites that, at any given time, are in one of a few possible states. In most ecological applications a site is either empty (state = $\mathbf{0}$) or occupied by a single individual of species i (state = i); lattice epidemic models (e.g. Filipe & Gibson, 1998; Kleczkowski *et al.*, 1997; Levin & Durrett, 1996; Rhodes & Anderson, 1996; Sato *et al.*, 1994) typically have one individual per site, classified by disease state. Each individual interacts with a limited number of neighbors, such that transition rates at a site are a function of the states of the site and its neighbors (Durrett, 1999). Most applications have used a rectangular lattice with a site’s neighborhood being either the eight surrounding sites or the four sites directly above, below and to the side,



but other geometries and randomly linked lattices have also been considered (van Baalen, 2000).

PA is a moment closure method which produces a system of ordinary differential equations for the frequency of each type of neighboring site pairs, e.g., the fraction of neighboring sites in which both are empty. Higher-order frequencies (e.g. for triplets) are approximated by pair frequencies in order to obtain a closed system of equations (Rand, 1999). The equations are nonlinear but fairly low dimensional. As a result PA has been applied successfully to models for a wide range of phenomena, including host–pathogen dynamics, multiple modes of reproduction in plants, forest gap dynamics, evolution of altruism, bacterial allelopathy, and cell sorting (see Iwasa (2000) for a review), and similar methods have been developed for epidemic models with “neighbors” defined by social interactions (Keeling, 1999a, b; Keeling *et al.*, 1997).

Related moment-closure methods have recently been developed for models in continuous space where the exact location of each individual is tracked. Interaction strengths are assumed to decrease as a function of the distance between individuals and are modeled by continuous kernel functions (e.g. Bolker, B. & Pacala, 1997; Bolker, 1999; Bolker, B. M. & Pacala, 1999; Law & Dieckmann, 2000a; Mollison, 1997). For example, a dispersal kernel $m(x, y)$ can be used to define the probability density of the landing point y for seeds produced by a parent at location x , and a competition kernel $w(x, y)$ to define the amount by which an individual at location y increases the mortality rate of an individual at location x . Each type of interaction has its own kernel and consequently its own spatial scale; for example, individuals too far apart to compete for resources may still be close enough for disease transmission via an animal vector. This representation of spatial effects is more realistic than a lattice model, but the resulting moment equations are partial- or integro-differential equations, which are less tractable than the ODE moment equations in PA.

Models of virulence evolution in host–pathogen interactions illustrate the need for extending PA to consider multiple spatial scales of interaction. Boots & Sasaki (1999, 2000) analysed lattice models with a combination of local and global interactions for host reproduction and infection, local referring to interaction with nearest

neighbors, global referring to interaction with all individuals regardless of location. Scaling between local and global interactions was modeled by a weighted averaging of the two options, so that (for example) a fraction P of offspring are dispersed to neighboring sites while the remaining $1-P$ are dispersed randomly over the entire lattice. Depending on the relative importance of local vs. global interactions in reproduction and infection, the level of virulence could evolve to levels very different from those in either the completely local or completely global models. Multiple interaction scales can also become important in multispecies ecological models, where an advantage in long-range dispersal can allow a competitively inferior species to persist (Neuhauser, 1998), or where short-range dispersal can allow a species to persist by quickly exploiting the available resources in a newly colonized area (Bolker & Pacala, 1999).

In this paper I explain how PA can be extended so that different interactions can occur over different finite spatial scales, by using a different neighborhood definition for each type of interaction. The method is to apply the PA moment closure simultaneously on the two different scales, so I refer to it as the “multiscale pair approximation” (MPA). The moment equations are very similar to standard PA, but there are more of them because each neighborhood type requires its own equations.

To show that the resulting moment equations remain tractable, I apply MPA to a lattice logistic model corresponding to the continuous-space model in (Bolker & Pacala, 1997; Law & Dieckmann, 2000b). Nearly identical models are considered in these two papers—henceforth called BP97 and LD00—and all statements here about the continuous space logistic model are taken from either or both of those papers. Numerical solutions of the moment equations for the continuous-space model showed that the steady-state population density could be higher or lower than in the non-spatial case (mean-field approximation), depending on the relative sizes of the competition and offspring dispersal neighborhoods. In the MPA for the lattice model this result can be derived analytically, and it is also possible to determine how the magnitude of the effect (fractional increase or decrease relative to

mean field) depends on other model parameters. These qualitative predictions are all confirmed by simulations.

2. Pair Approximation for a Lattice Logistic Model

I consider a lattice model analogous to the continuous-space logistic model in BP97 and LD00, in which adults are sessile and have a mortality rate affected by local crowding. Bolker *et al.* (2000) considered a slightly different situation where local crowding affects the establishment success of offspring, while Law & Dieckmann (2000a) allowed movement by established individuals. These features could be incorporated here, under assumptions of linear density effects similar to those in the continuous-space models, but are omitted to simplify the presentation. I assume a rectangular lattice, but allow any neighborhood shape such that neighborhood relations are symmetric: if site y is in the neighborhood of site x , then site x must be in the neighborhood of site y , so that any pair of sites is either neighboring or non-neighboring.

Each site in the lattice model is either empty (state = $\mathbf{0}$), or else occupied by one individual of the focal species (state = $\mathbf{1}$). Thus, all non-spatial aspects of population structure are ignored, as in the continuous-space model. Each occupied site produces offspring at rate b , meaning that in a small time interval dt the probability that an offspring is produced is $b dt + o(dt)$. Each new offspring is dispersed into one of z sites in the *birth neighborhood* of the parent’s site, chosen at random and independent of the state of the lattice; if that site is empty it becomes occupied, and if it is already occupied it remains occupied. An occupied site dies (becomes empty) at rate

$$1 + \delta \times \{ \# \text{ occupied sites in the } \textit{competition neighborhood} \}. \quad (1)$$

Note that time has implicitly been scaled so that the instantaneous mortality rate of an isolated individual is 1. The number of sites in the competition neighborhood of a focal site is denoted by \bar{z} . Let β denote the birth rate per site ($\beta = b/z$, the rate at which an empty site receives offspring

from an occupied neighbor), and let d denote the maximum possible density-dependent increase in an individual's death rate ($d = \delta\tilde{z}$). The time-rescaled model is, therefore, defined by four parameters: b and d giving the total interaction effects over the relevant neighborhood, and z and \tilde{z} giving the spatial range of the interactions.

Consider first pair approximation for the standard case where the birth and competition neighborhoods are the same (so $\tilde{z} = z$); for a complete account of pair approximation theory see (Rand, 1999; van Baalen, 2000). Let ρ_i denote the frequency of type- i sites, and ρ_{ij} the frequency of neighboring pair sites in which the first is type i and the second is type j , $i, j \in \{0, 1\}$. For readers new to PA it may be useful to give the following heuristic definition of pair frequencies. Choose a site at random, and then choose a random neighbor of that first site. The probability that the first site chosen is type i , and that the random neighboring site is type j , is ρ_{ij} . The conditional probability that the neighbor is of type j , given that the first-chosen site is type i , is denoted $q_{j|i}$; therefore $q_{j|i} = \rho_{ij}/\rho_i = \rho_{ji}/\rho_j$.

A site in state **1** changes to state **0** at the rate given in eqn (1). The average rate over all such sites is, therefore, $1 + \delta \times \{\text{expected number of occupied neighbor sites}\} = 1 + \delta z q_{1/1} = 1 + d q_{1/1}$, and the total rate over all such sites is $(1 + d q_{1/1})\rho_1$. Similarly, the total rate of transitions between state **0** and state **1** is $\beta z q_{1/0} \rho_0 = b q_{1/0} (1 - \rho_1)$, and therefore

$$\frac{d\rho_1}{dt} = b q_{1/0} (1 - \rho_1) - (1 + d q_{1/1}) \rho_1. \quad (2)$$

Note that the derivation of eqn (2) did not involve any approximations—it is exactly true, but it is not closed because it involves the pair frequencies $q_{1/0} (1 - \rho_1) = \rho_{10}$ and $q_{1/1} \rho_1 = \rho_{11}$. The non-spatial (mean-field) approximation to the lattice model is obtained by ignoring all correlations between neighboring sites, and replacing $q_{1/i}$ in eqn (2) by the unconditional probability of a site being in state **1**, namely ρ_1 . This yields

$$\frac{d\rho_1}{dt} = (b - 1)\rho_1 - (b + d)\rho_1^2 \quad (3)$$

which is a single-species logistic equation.

In pair approximation we stick with eqn (2) and add equations for the dynamics of pair frequencies. There are four pair frequencies ρ_{ij} , $i, j \in \{0, 1\}$, but the constraints $\sum \rho_{ij} = 1$, $\rho_{01} = \rho_{10}$ mean that only two of these are independent. It is convenient to keep $\rho_1 = \rho_{11} + \rho_{10}$ as one of the state variables and take ρ_{11} as the second. A pair of sites in state **11** can change to either **10** or **01**. The rate for each of these transitions is the death rate for an occupied site with an occupied neighbor, which we approximate as

$$1 + \delta[1 + (z - 1)q_{1/1}]. \quad (4)$$

The “1” inside the square braces is the contribution from the occupied neighbor. The second term is *approximately* the expected number of occupied sites in the other $(z - 1)$ neighboring sites. The approximation is that $q_{1/1}$ is used as the probability that another neighbor of the focal site is occupied, ignoring the additional information that the focal site is known to have at least one occupied neighbor. This is the pair approximation: we ignore all spatial correlations except between neighboring site pairs. Similarly, new pairs of type **11** result from births into the unoccupied site of **01** and **10** pairs. Those rates are approximated as

$$\beta[1 + (z - 1)q_{1/0}] \quad (5)$$

which yields the (approximate) equation for the frequency of **11** pairs,

$$\begin{aligned} \frac{1}{2} \frac{d\rho_{11}}{dt} &= \beta[1 + (z - 1)q_{1/0}] \rho_{10} \\ &- (1 + \delta[1 + (z - 1)q_{1/1}]) \rho_{11}. \end{aligned} \quad (6)$$

Using the relationship $\rho_{10} = \rho_1 - \rho_{11}$ and recalling the definition of the conditional probabilities ($q_{ij} = \rho_{ij}/\rho_j$) it is seen that eqns (2) and (6) are a closed system, which comprise the pair approximation for the case $z = \tilde{z}$.

3. Multiscale Pair Approximation

If the birth and competition neighborhoods are different, PA has to be extended by deriving

separate equations for the two neighborhood types. In this section I derive this multiscale pair approximation for a single-species lattice model with two types of interaction neighborhoods, and Section 4 returns to the lattice logistic model with nested birth and death neighborhoods. Three or more neighborhoods can be handled in exactly the same way, so this generalization is omitted. For simplicity I consider linear interaction effects; methods for nonlinear effects are discussed by van Baalen (2000).

Each site is assumed to have two disjoint neighborhoods, which will be called “near” and “far” neighbors although the neighborhood definitions need not be based on a distance function. The use of disjoint neighborhoods as a device for handling nested interaction neighborhoods is the one essential new idea in MPA, which makes it possible to apply PA simultaneously on two scales. The sizes of the near and far neighborhoods are denoted z_n and z_f , respectively. The definitions of pair frequencies and conditional probabilities used in pair approximation are applied to each type of neighborhood, with $\tilde{\rho}_{ij}$ and $\tilde{q}_{j|i}$ for far-neighbor pairs and ρ_{ij} , $q_{j|i}$ referring to near-neighbor pairs. There are now eight different pair frequencies, but the following five constraints hold:

$$\begin{aligned} \sum \rho_{ij} &= \sum \tilde{\rho}_{ij} = 1, \\ \rho_{10} &= \rho_{01}, \quad \tilde{\rho}_{10} = \tilde{\rho}_{01}, \\ \rho_{00} + \rho_{01} &= \tilde{\rho}_{00} + \tilde{\rho}_{01}. \end{aligned} \tag{7}$$

In the last line, the common value of the two sums is ρ_0 . The corresponding constraint for ρ_1 is also true, but it is not an additional constraint because it can be derived from eqn (7). Consequently, there are three independent pair frequencies, and to parallel the single-neighborhood case I choose ρ_1 , ρ_{11} , $\tilde{\rho}_{11}$ as the state variables.

Generalizing the lattice logistic model described above, the death rate of an occupied site is assumed to be

$$\begin{aligned} &1 + \delta_n \times \{ \# \text{ occupied near-neighbor sites} \} \\ &+ \delta_f \times \{ \# \text{ occupied far-neighbor sites} \}. \end{aligned} \tag{8}$$

In a similar way, an occupied site disperses offspring at different rates β_n , β_f onto its near and far neighborhoods, respectively. The total birth rate for an unoccupied site is, therefore, given by

$$\begin{aligned} &\beta_n \times \{ \# \text{ occupied near-neighbor sites} \} \\ &+ \beta_f \times \{ \# \text{ occupied far-neighbor sites} \}. \end{aligned} \tag{9}$$

For comparison with the single-neighborhood case, define $b = \beta_n z_n + \beta_f z_f$ (the total birth rate by an occupied site onto all neighbors) and $d = \delta_n z_n + \delta_f z_f$ (the maximum possible density-dependent death rate increment).

The equation for ρ_1 is derived exactly as in the single-neighborhood case, except that the birth and death rates involve contributions from near and far neighbors. Equation (2) is consequently generalized to

$$\begin{aligned} \frac{d\rho_1}{dt} &= (\beta_n z_n q_{1/0} + \beta_f z_f \tilde{q}_{1/0})(1 - \rho_1) \\ &- (1 + \delta_n z_n q_{1/1} + \delta_f z_f \tilde{q}_{1/1})\rho_1. \end{aligned} \tag{10}$$

The corresponding mean-field approximation is again obtained by replacing $q_{1/0}$ and $\tilde{q}_{1/1}$ by the unconditional frequency of occupied sites ρ_1 , which gives

$$\frac{d\rho_1}{dt} = (b - 1)\rho_1 - (b + d)\rho_1^2. \tag{11}$$

Thus, the mean-field approximation is the same as in the single-neighborhood case [eqn (3)] with the same steady-state population density $\bar{\rho}_1 = (b - 1)/(b + d)$.

To derive the approximate pair frequency equations, consider first the rate at which a death converts a **11** near-neighbor pair into a **10** or **01** pair. Each member of the pair is known to have one near neighbor, but nothing is known directly about the number of far neighbors. The death rate (for either one of the occupied sites in the pair) is therefore approximated as

$$1 + \delta_n(1 + (z_n - 1)q_{1/1}) + \delta_f z_f \tilde{q}_{1/1}. \tag{12}$$

Similarly for births converting a **10** or **01** near-neighbor pair to a **11** pair, the approximate birth

rate for the unoccupied site is

$$\beta_n(1 + (z_n - 1)q_{1/0}) + \beta_f z_f \tilde{q}_{1/0}. \quad (13)$$

In these rate equations for near-neighbor pair frequencies, PA is applied as usual for the contributions for near neighbors: the state of the focal site's known near neighbor is ignored in computing the conditional probability (conditioned on the state of the focal site) for other near-neighbor sites. For the contributions from far neighbors, the state of the known near neighbor is ignored for computing the conditional probability for all far-neighbor sites. Because the near and far neighborhoods are disjoint, this is just a second application of the PA moment closure. Combining eqns (12) and (13) we have

$$\begin{aligned} \frac{1}{2} \frac{d\rho_{11}}{dt} &= [\beta_n(1 + (z_n - 1)q_{1/0}) + \beta_f z_f \tilde{q}_{1/0}] \rho_{10} \\ &\quad - [1 + \delta_n(1 + (z_n - 1)q_{1/1}) \\ &\quad + \delta_f z_f \tilde{q}_{1/1}] \rho_{11}. \end{aligned} \quad (14)$$

By identical arguments the equation for **11** far-neighbor pairs is derived as

$$\begin{aligned} \frac{1}{2} \frac{d\tilde{\rho}_{11}}{dt} &= [\beta_f(1 + (z_f - 1)\tilde{q}_{1/0}) + \beta_n z_n q_{1/0}] \tilde{\rho}_{10} \\ &\quad - [1 + \delta_f(1 + (z_f - 1)\tilde{q}_{1/1}) \\ &\quad + \delta_n z_n q_{1/1}] \tilde{\rho}_{11}. \end{aligned} \quad (15)$$

Using the relationships $\rho_0 = 1 - \rho_1$, $\rho_{10} = \rho_1 - \rho_{11}$ and the parallel ones for far-neighbor pairs, eqns (10), (14), and (15) are seen to be a closed system of equations.

It is useful to express the system in terms of total interaction effects over the neighborhood. Define

$$\begin{aligned} \varepsilon_n &= 1/z_n, & b_n &= \beta_n z_n, & d_n &= \delta_n z_n, \\ \varepsilon_f &= 1/z_f, & b_f &= \beta_f z_f, & d_f &= \delta_f z_f. \end{aligned} \quad (16)$$

The ε 's can generally be thought of as small parameters, since $\varepsilon \ll 1$ already for $z = 8$. The

moment equations can then be written as

$$\frac{d\rho_1}{dt} = (b - 1)\rho_1 - (b_n + d_n)\rho_{11} - (b_f + d_f)\tilde{\rho}_{11}, \quad (17a)$$

$$\begin{aligned} \frac{1}{2} \frac{d\rho_{11}}{dt} &= \left[b_n \left(\varepsilon_n + (1 - \varepsilon_n) \frac{\rho_1 - \rho_{11}}{1 - \rho_1} \right) \right. \\ &\quad \left. + b_f \frac{\rho_1 - \tilde{\rho}_{11}}{1 - \rho_1} \right] (\rho_1 - \rho_{11}) \\ &\quad - \left[1 + d_n \left(\varepsilon_n + (1 - \varepsilon_n) \frac{\rho_{11}}{\rho_1} \right) \right. \\ &\quad \left. + d_f \frac{\tilde{\rho}_{11}}{\rho_1} \right] \rho_{11}, \end{aligned} \quad (17b)$$

$$\begin{aligned} \frac{1}{2} \frac{d\tilde{\rho}_{11}}{dt} &= \left[b_f \left(\varepsilon_f + (1 - \varepsilon_f) \frac{\rho_1 - \tilde{\rho}_{11}}{1 - \rho_1} \right) \right. \\ &\quad \left. + b_n \frac{\rho_1 - \rho_{11}}{1 - \rho_1} \right] (\rho_1 - \tilde{\rho}_{11}) \\ &\quad - \left[1 + d_f \left(\varepsilon_f + (1 - \varepsilon_f) \frac{\tilde{\rho}_{11}}{\rho_1} \right) \right. \\ &\quad \left. + d_n \frac{\rho_{11}}{\rho_1} \right] \tilde{\rho}_{11}. \end{aligned} \quad (17c)$$

In this form, the spatial scale and the intensity of interspecific interactions are controlled by separate sets of parameters (the ε 's vs. the b 's and d 's, respectively).

Figure 1(a) shows two comparisons between simulation results and numerical solutions of the MPA equations (17). The first case (circles) had relatively small neighborhoods (near = 3×3 square, far = 5×5 square minus the near neighbors); the second (squares) had relatively large neighborhoods (near = 5×5 , far = 9×9 minus the near neighbors). In these cases the differences between the simulated and approximate trajectories are trivial. However, these cases both had fairly high values of the total birth rate ($b = 6$ and 3 , respectively), and it is known that the relative error of the ordinary PA increases when the birth

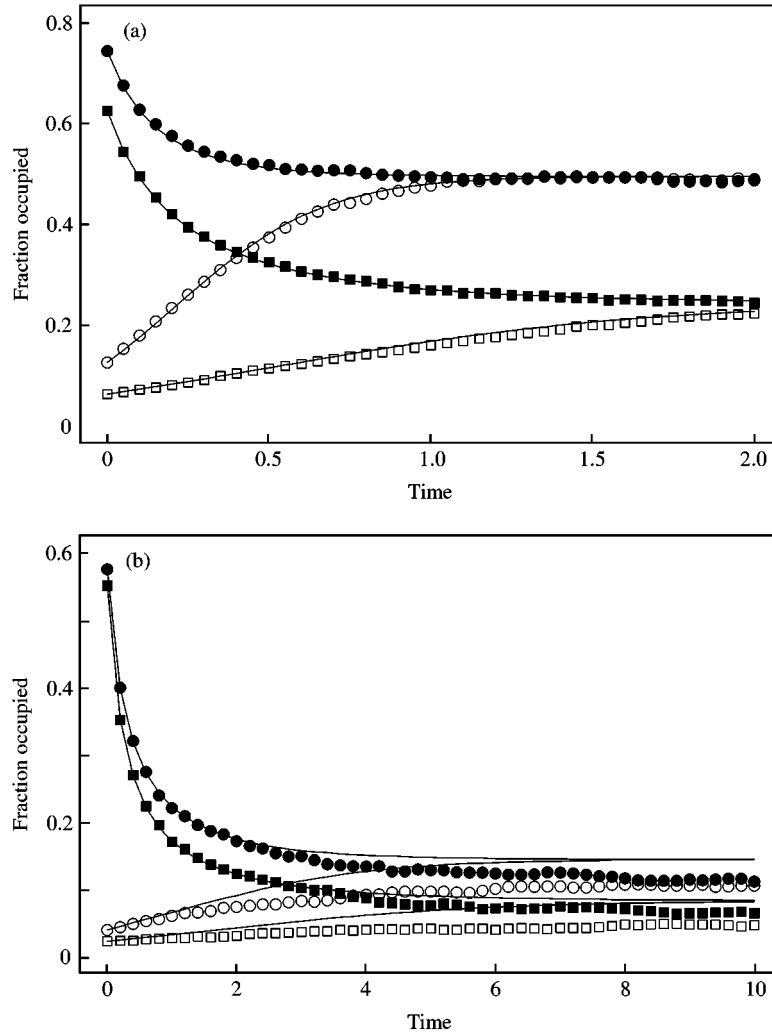


FIG. 1. Comparison between numerical solutions of the MPA differential equations (17) [solid lines] and simulations of the model [symbols]. The model was simulated in discrete time with time step $dt = 0.001$, starting from a spatially random initial state, on a 150×150 lattice with wrap-around boundary conditions. Initial lattice states were generated by independently assigning each site as empty or occupied, with probability equal to either 25% of the mean-field steady-state value (open symbols) or to halfway between 1 and the mean-field steady-state value (solid symbols). Initial conditions for the MPA equations were $\rho_1(0)$ set equal to the fraction of occupied sites in the initial state of the simulation, and $\rho_{11}(0) = \tilde{\rho}_{11}(0) = \rho_1(0)^2$, corresponding to a spatially uncorrelated lattice. The neighborhoods used in the simulations were nested squares, as described in the text. (a) Parameter values were $(b_n, b_f, d_n, d_f) = (3, 3, 2, 2)$ and $(2, 1, 4, 1)$ for the simulations plotted with circles and squares, respectively, with neighborhood sizes $(z_n, z_f) = (8, 16)$ and $(24, 56)$, respectively. (b) As in panel (a) but with birth rates scaled down proportionately to give $b = 2$ in both cases: $(b_n, b_f) = (1, 1)$ and $(4/3, 2/3)$ for the simulations plotted with circles and squares, respectively.

rate is close to the critical value for persistence. MPA inevitably inherits this limitation. Figure 1(b) repeats the simulations in Fig. 1(a) but with the β 's scaled down proportionally so that $b = 2$ in both cases, and the differences are more substantial. The approach to steady state is slower, and as expected the MPA equations over-predict the steady-state value and therefore diverge eventually from the simulated trajectories.

However, the absolute error in MPA predictions is still not very large, and MPA correctly identifies which parameter set has the larger steady-state density.

4. Large Neighborhood Limits

In the limit of both interaction scales becoming infinitely large ($\varepsilon_n, \varepsilon_f \rightarrow 0$), MPA reduces to the

mean-field approximation. The two equations for pair frequencies become identical, so if we start with a spatially random lattice (i.e. $\rho_{11} = \tilde{\rho}_{11} = \rho_1^2$) it remains true for all time that $\rho_{11} = \tilde{\rho}_{11}$ and the system reduces to

$$\begin{aligned} \frac{d\rho_1}{dt} &= (b-1)\rho_1 - (b+d)\rho_{11}, \\ \frac{1}{2} \frac{d\rho_{11}}{dt} &= b \frac{(\rho_1 - \rho_{11})^2}{1 - \rho_1} - \left(1 + d \frac{\rho_{11}}{\rho_1}\right) \rho_{11}. \end{aligned} \quad (18)$$

Moreover, direct substitution shows that a solution of eqn (18) is obtained by solving the mean-field equation (11) for ρ_1 and setting $\rho_{11} = \rho_1^2$. If the initial state of the lattice is spatially non-random (e.g. if all occupied sites are near neighbors), the initial spatial correlations will persist transiently but eqn (18) asymptotically converges to the spatially random steady state with the mean-field steady-state density $\bar{\rho}_1 = (b-1)/(b+d)$ and $\rho_{11} = \rho_1^2$. Thus, a general prediction of MPA for this model is that the steady-state departures from mean field will be of order $(\varepsilon_n + \varepsilon_f)$.

A more interesting case is to let $\varepsilon_f \rightarrow 0$ but retain $\varepsilon_n > 0$. Then direct substitution shows that eqn (17) is satisfied by setting $\tilde{\rho}_{11} = \rho_1^2$ and solving the first two equations with this substitution. With $\varepsilon_f = 0$ and $\tilde{\rho}_{11} = \rho_1^2$, the first two equations can be expressed as

$$\begin{aligned} \frac{d\rho_1}{dt} &= \rho_1 [b-1 - (b_n + d_n)q_{1/1} - (b_f + d_f)\rho_1], \\ \frac{1}{2} \frac{d\rho_{11}}{dt} &= \rho_{01} [b_n(\varepsilon_n + (1 - \varepsilon_n)q_{1/0}) \\ &\quad + b_f \rho_1] (\rho_1 - \rho_{11}) \\ &\quad - \rho_{11} [1 + d_n(\varepsilon_n + (1 - \varepsilon_n)q_{1/1}) + d_f \rho_1]. \end{aligned} \quad (19)$$

The near-neighbor effects (b_n, d_n) are still determined by the local crowding ($q_{1/i}$) as in ordinary PA, but the far-neighbor effects (b_f, d_f) are

proportional to the global density of occupied sites. Thus, if the longer interaction scale becomes infinite ($\varepsilon_f \rightarrow 0$), MPA reduces to ordinary PA for a model with a weighted mixture of local and global interactions. For $0 < \varepsilon_f \ll 1$, the difference between MPA and eqn (19) is of order ε_f .

5. Multiscale Lattice Logistic Model

I now specialize these results to the lattice logistic model with birth and competition neighborhoods of different size, for comparison with the corresponding continuous-space model (BP97, LD00). Recall that the lattice logistic model has birth and competition neighborhoods of sizes z and \tilde{z} , respectively, with constant per-site rates across these neighborhoods. In terms of the more general MPA in Sections 3 and 4, we therefore have either

$$z < \tilde{z}: \quad \beta_f = 0, \delta_n = \delta_f, \quad (20)$$

$$z > \tilde{z}: \quad \delta_f = 0, \beta_n = \beta_f \quad (21)$$

or

$$z = \tilde{z}: \quad \delta_f = \beta_f = 0. \quad (22)$$

In cases (20) and (21) the near- and far-neighborhood sizes are $z_n = \min(z, \tilde{z})$, $z_f = |z - \tilde{z}|$.

In case (22) MPA reduces to ordinary PA. A standard result for this case is that local crowding reduces the steady-state density below the mean-field value $\bar{\rho}_1 = (b-1)/(b+d)$, and therefore increases the critical birth rate for persistence ($b > 1$ is therefore always necessary for persistence, and we assume this to be true). For the continuous-space model, the effect of spatial pattern on steady-state density depends on the relative spatial scales of offspring dispersal and competition (see Fig. 6 of BP97). If births are more localized than competition [corresponding to case (20)], then the effect of local crowding on birth rate continues to depress the steady-state density below the mean-field value. However, if competition is localized but offspring are widely dispersed [corresponding to case (21)], then individuals are more widely separated than under a spatially random distribution and as a result the steady-state density is higher than the mean-field value.

These results for the continuous-space model were inferred from numerical solution of steady-state moment equations. For the lattice model we can derive some predictions by treating the ε 's as small parameters in eqn (17) and perturbing off the mean-field steady state which holds at $\varepsilon = 0$. The full expansion for eqn (17) is complicated but can be interpreted by considering some specific cases (see the appendix). The most interesting case is eqn (21) with widely dispersed offspring but localized competition ($z \gg \tilde{z}$, hence $\varepsilon_f \ll \varepsilon_n = 1/\tilde{z} \ll 1$). Neglecting $O(\varepsilon_f)$ terms, the approximate steady-state fraction of occupied sites is

$$\bar{\rho}_1 \doteq \bar{\rho}_1(0) \left(1 + \tilde{z}^{-1} \left[\frac{d^2(1+d)}{b(b+d)^2} \right] \right), \quad (23)$$

where $\bar{\rho}_1(0)$ is the mean-field steady-state density. In contrast, for equal neighborhood sizes [case (22)], ε_f disappears from the equations and the first-order expansion is

$$\bar{\rho}_1 \doteq \bar{\rho}_1(0) \left(1 - \tilde{z}^{-1} \left[\frac{(1+d)}{b(b-1)} \right] \right). \quad (24)$$

Similarly, for the case (21) of localized offspring dispersal but long-range competitive interactions ($z \ll \tilde{z}$, hence $\varepsilon_f \ll \varepsilon_n = 1/z \ll 1$), the leading order expansion is

$$\bar{\rho}_1 \doteq \bar{\rho}_1(0) \left(1 - z^{-1} \left[\frac{(1+d)^2 b}{(b+d)^2 (b-1)} \right] \right). \quad (25)$$

The steady-state density is depressed below the mean-field level, with the relative decrease being larger as the range of offspring dispersal shrinks.

Comparing the three expansions above for $\bar{\rho}_1$ we obtain several predictions for how the steady-state density is affected by the spatial range of interactions:

- (1) As the size of the birth neighborhood increases to become larger than the competition neighborhood
 - (a) The steady-state density crosses from below to above the mean-field value.
 - (b) The relative departures from mean field, both above and below, should be larger at higher values of the death rate increment d , and smaller at higher birth rate b .

- (2) With a large birth neighborhood of fixed size $z \gg 1$, as the size of the competition neighborhood \tilde{z} is increased from $\tilde{z} \ll z$ to $\tilde{z} \approx z$, the steady state should decrease from above to slightly below the mean-field value.

Prediction (1) also holds in the moment equations for the continuous space model (BP97, Fig. 6), but prediction (2) does not because the continuous-space moment equations break down due to infinite clustering in the limit of large competition range (BP97, p. 188). In the lattice model clustering is limited by the finite size of cells imposing a minimum distance between individuals.

To test these predictions I simulated the lattice model using square birth and competition neighborhoods centered on the focal site. Formally, the neighborhood of radius $r = 1, 2, 3, \dots$ for a site (i, j) consists of all sites (k, l) such that $0 < \max\{|i - k|, |j - l|\} \leq r$, and contains $(2r + 1)^2 - 1$ cells. The simulation results shown in Fig. 2 are all in agreement with prediction (1) as b, d , and the size of the birth neighborhood are varied. Prediction (2) is also confirmed in simulations. For example in a series of simulations (not graphed) starting with $b = 2, d = 5$ and a birth neighborhood of radius 6 (i.e. the farthest-right square in the top panel of Fig. 2), as the radius of the competition neighborhood was increased from $r = 1$ to 6, the steady-state density went from 11% above, to 7% below, the mean-field density.

The effects of neighborhood size (with b and d held constant) can be summarized as follows. If the birth and competition neighborhoods are both large [eqn (24) with $\tilde{z} \rightarrow \infty$], the steady-state population density will be at the mean-field value. Decreasing the size of the competition neighborhood increases the steady-state density [eqn (23)] while decreasing the size of the birth neighborhood decreases the population size [eqn (25)]. As in the continuous space model, the effects of neighborhood size are due to changes in the spacing pattern of individuals (Fig. 3). When the birth and competition neighborhoods are both large ($r = 6, 138$ sites) the density is at the mean-field level, $\bar{\rho}_1(0) = 0.25$. Decreasing the size of the competition neighborhood to $r = 1$ increases the density slightly to $\bar{\rho}_1 = 0.27$ (by

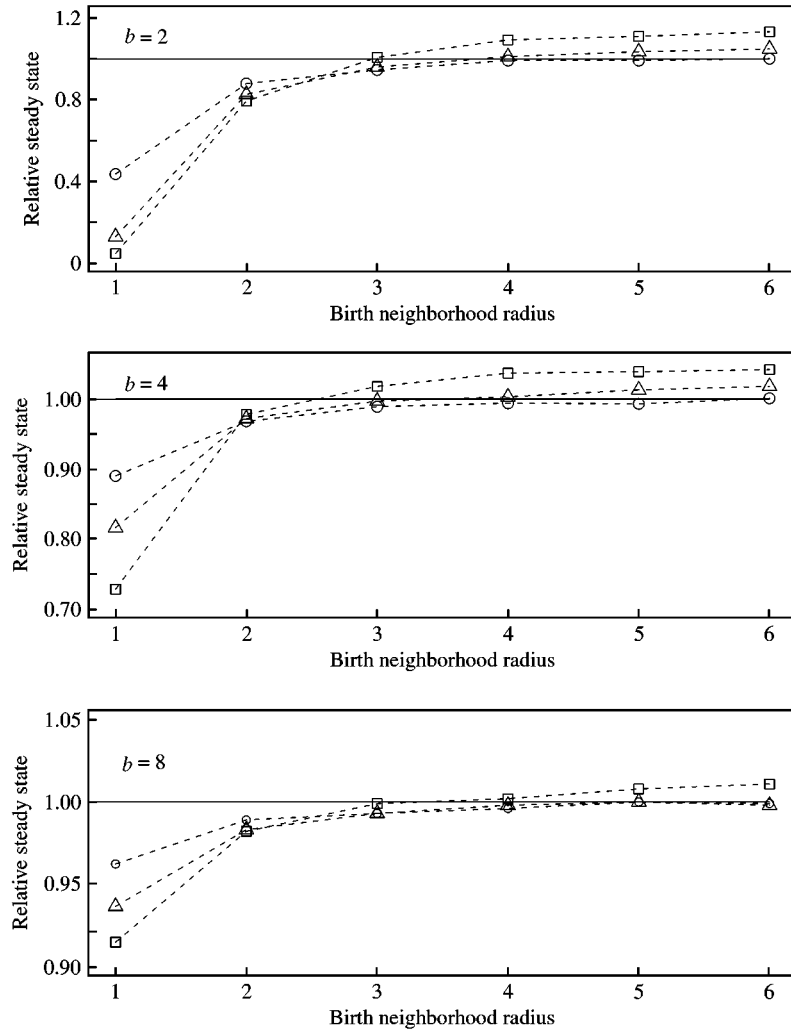


FIG. 2. Results from simulations testing the qualitative predictions of MPA about steady-state population density as a function of birth neighborhood size in the lattice logistic model. Values plotted are the ratio between the steady-state density estimated by simulation and the mean-field steady-state density $\bar{\rho}_1 = (b - 1)/(b + d)$; the solid line is at ratio = 1. All simulations used a competition neighborhood of radius $r = 1$ (eight neighbors). The steady-state density was estimated by initializing the lattice to the mean-field steady state as described in the Fig. 1 legend, allowing the model to run for 10 time units (time is scaled so that 1 time unit is the mean lifetime for isolated individual), and then averaging the fraction of occupied sites at each 0.1 time units between times 10 and 15. (○) $d = 1$; (△) $d = 3$; (□) $d = 5$.

slightly increasing the average spacing between individuals), while shrinking the birth neighborhood to radius $r = 1$ promotes clustering of individuals and consequently the overall density is reduced ($\bar{\rho}_1 = 0.19$). For these parameter values, comparison of eqns (24) and (25) predicts that the population density will be lowered further if both neighborhoods are reduced to $r = 1$, as is observed ($\bar{\rho}_1 = 0.17$).

The overall conclusion is that the qualitative effects of interaction scales and endogenously generated spatial pattern are very similar in the

lattice and continuous space versions of the model, and are successfully predicted by MPA for the lattice model.

6. Discussion

Numerically accurate results for stochastic spatial models can always be obtained by simulation, and if accurate numbers are needed (e.g. for rates of population growth or spread) the proper approach is simulation rather than PA or other approximations. The value of approximations is

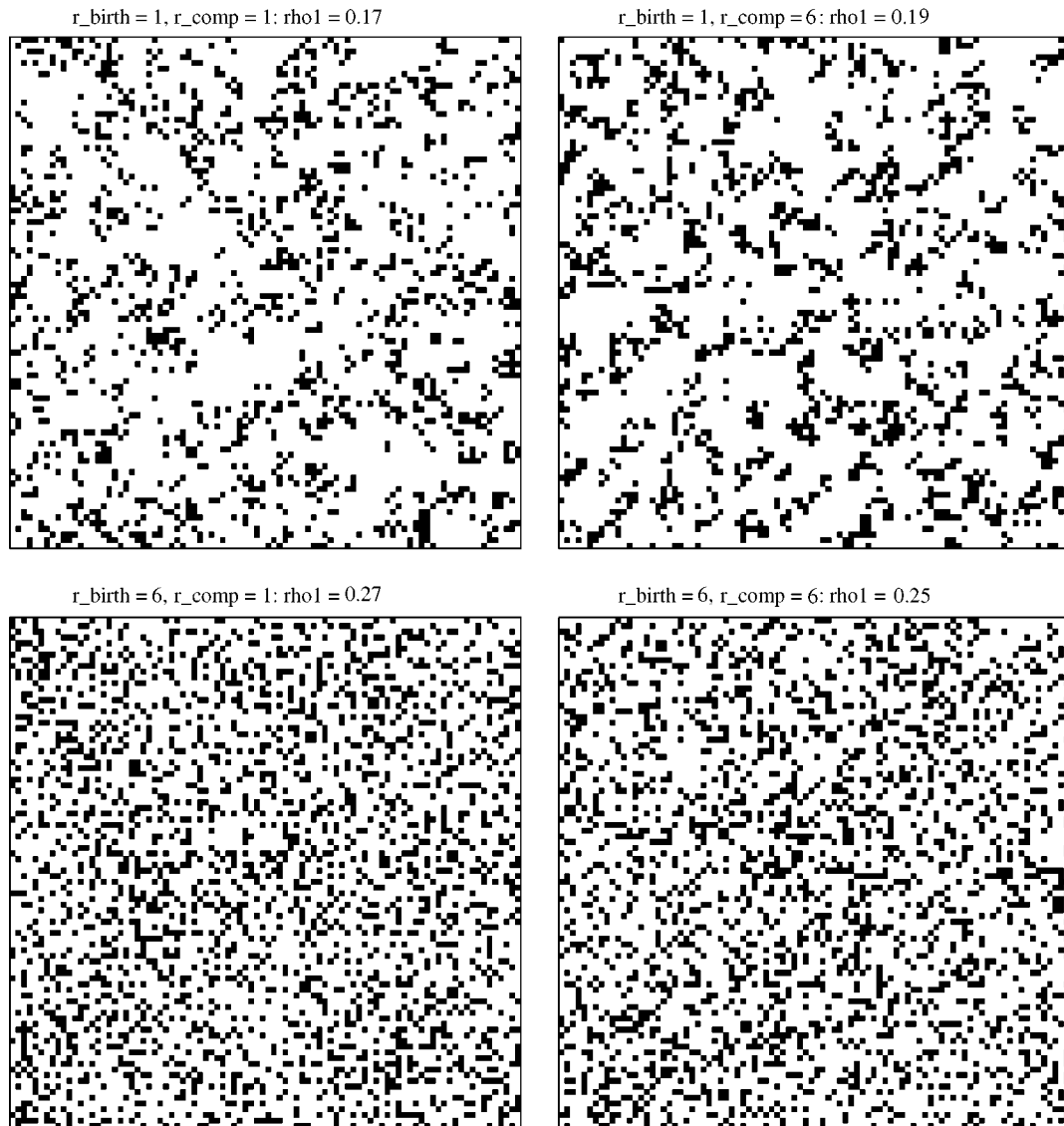


FIG. 3. Snapshots of the lattice logistic model at steady state, to show how the spatial pattern of occupied sites (black squares) is affected by the size of the birth and competition neighborhoods. The plots show a 90×90 square at time $t = 10$ from a lattice of size 150×150 , initialized and simulated as in Fig. 1, with $b = 3$ and $d = 5$. The steady-state density in the mean-field approximation is 0.25.

not that they replace simulations, but that they can help us to understand the important qualitative properties of a model that are seen in simulations (van Baalen, 2000), and to predict the range of possible qualitative behaviors (Sato *et al.*, 1994). The fact that MPA is reasonably accurate for the lattice logistic model provides some support for the general approach, but it is more important that the approximation makes the correct qualitative predictions about the effects of interaction scales on the steady-state density, and

about how the magnitude of the effects depends on model parameters. In other words, MPA predictions of parameter effects are useful because they consistently get the sign right, and they are accurate enough to guide the choice of parameter values for simulations.

From that perspective, the main contribution of this paper may be the large-neighborhood limits (Section 4), because they provide a rationale and rough error estimates for the simpler approach of mixing local and global interactions.

According to those results, the difference at steady state between a longer-range interaction across a neighborhood of size z and a global interaction across the entire population is of order $1/z$. Consequently, it may be accurate enough to approximate all but the shortest-range interactions by a global interaction, eliminating the extra moment equations for a longer-range interaction neighborhood. In a single-species model this only eliminates one moment equation, but in multispecies models it will eliminate several. Evolutionary models are unavoidably “multispecies” (competing genotypes, or invading and resident strategies), so a reduction in the number of moment equations will make the analysis considerably easier.

That such a drastic simplification of the interaction “kernels” has only minor effects on the dynamics of the PA moment equations is an indication that the properties captured by PA are not sensitive to the tails of the kernels. PA-type approximations are, therefore, not going to be useful when the properties of interest are sensitive to the tails, for example the expansion rate and shape of a wave or the focus of invasion by a species with long-range offspring dispersal. Continuous-space models, where the dispersal and competition kernels can be modeled in full detail, would then be more appropriate. However, our results suggest that steady-state properties can be analysed, at least qualitatively but with a great increase in tractability, by PA-type approaches to lattice models. As Hiebeler (1997) has argued, it is useful to have a continuum of approximations to fill in the gap between a non-spatial, deterministic mean-field approximation, and simulations of a spatially explicit, individual-based stochastic model. MPA allows much of the flexibility of the continuous-space approach to be incorporated into a lattice model without greatly increasing the complexity of the moment equations. As such, it may be a useful intermediate between the single interaction scale allowed in PA and a complete (but less tractable) set of moment equations for interactions and correlations at all spatial scales.

As one possible application, the problem motivating this paper was regional-scale modeling of *Aspergillus sydowii*, a fungal pathogen affecting sea fan corals (*Gorgonia* spp.) in the Caribbean.

First identified on corals in the mid-1990s, *Aspergillus* is now widespread throughout the Caribbean, causing up to 90% mortality on individual reefs (Kim & Harvell, 2001). There are three modes of infection with very different spatial scales: direct contact with a neighboring infected fan, local water-borne transmission, and fungus of terrestrial origin in runoff water or wind-borne dust. At the within-reef scale there is pronounced local clustering of infection (C. D. Harvell & K. Kim, unpublished data), indicating a need for spatial models incorporating local transmission, but it is not feasible to simulate such a model at the scale of the Caribbean basin. Using MPA moment equations as a reduced description of individual reefs, and coupling these into a regional-scale model, will facilitate computational studies of the factors affecting disease spread and severity, and comparisons of potential approaches for disease management in sessile marine species.

This work was supported by startup funds from the College of Arts and Sciences at Cornell University. I thank the referees and Matt Keeling for comments on the original manuscript.

REFERENCES

- BOLKER, B. & PACALA, S. W. (1997). Using moment equations to understand stochastically driven spatial pattern formation in ecological systems. *Theor. Popul. Biol.* **52**, 179–197.
- BOLKER, B. M. (1999). Analytic models for the patchy spread of plant disease. *Bull. Math. Biol.* **61**, 849–874.
- BOLKER, B. M. & PACALA, S. W. (1999). Spatial moment equations for plant competition: Understanding spatial strategies and the advantages of short dispersal. *Am. Nat.* **153**, 575–602.
- BOLKER, B. M., PACALA, S. W. & LEVIN, S. A. (2000). Moment methods for ecological processes in continuous space. In: *The Geometry of Ecological Interactions: Simplifying Spatial Complexity* (Dieckmann, U., Law, R. & Metz, J. A. J., eds), pp. 359–387. Cambridge: Cambridge University Press.
- BOOTS, M. & SASAKI, A. (1999). ‘Small worlds’ and the evolution of virulence: infection occurs locally and at a distance. *Proc. R. Soc. London Ser. B* **266**, 1933–1938.
- BOOTS, M. & SASAKI, A. (2000). The evolutionary dynamics of local infection and global reproduction in host–parasite interactions. *Ecol. Lett.* **3**, 181–185.
- DIECKMANN, U., LAW, R. & METZ, J. A. J., ed. (2000). *The Geometry of Ecological Interactions: Simplifying Spatial Complexity*. Cambridge: Cambridge University Press.
- DURRETT, R. (1999). Stochastic spatial models. *SIAM Rev.* **41**, 677–718.
- DURRETT, R. & LEVIN, S. (2000). Lessons on pattern formation from planet WATOR. *J. theor. Biol.* **205**, 201–214.

- FILIPE, J. A. N. & GIBSON, G. J. (1998). Studying and approximating spatio-temporal models for epidemic spread and control. *Philos. Trans. R. Soc. London Ser. B* **353**, 2153–2162.
- HIEBELER, D. E. (1997). Stochastic spatial models: from simulations to mean field and local structure approximations. *J. theor. Biol.* **187**, 307–319.
- IWASA, Y. (2000). Lattice models and pair approximation in ecology. In: *The geometry of ecological interactions: Simplifying spatial complexity* (Dieckmann, U., Law, R. & Metz, J. A. J., eds), pp. 227–251. Cambridge: Cambridge University Press.
- KEELING, M. (1999a). Correlation equations for endemic diseases: externally imposed and internally generated heterogeneity. *Proc. R. Soc. London Ser. B* **266**, 933–960.
- KEELING, M. (1999b). The effects of local spatial structure on epidemiological invasions. *Proc. R. Soc. London Ser. B* **266**, 859–867.
- KEELING, M., RAND, D. & MORRIS, A. (1997). Correlation models for childhood epidemics. *Proc. R. Soc. London Ser. B* **264**, 1149–1156.
- KIM, K. & HARVELL, C. D. (2001). Aspergillosis of sea fan corals: dynamics in the Florida Keys. In: *Connections Between Ecosystems in the South Florida Hydroscape: The River of Grass Continues* (Porter, J. W. & Porter, K., eds). Boca Raton, FL: CRC Press.
- KLECZKOWSKI, A., GILLIGAN, C. A. & BAILEY, D. J. (1997). Scaling and spatial dynamics in plant pathogen systems: from individuals to populations. *Proc. Trans. R. Soc. London Ser. B* **264**, 979–984.
- LAW, R. & DIECKMANN, U. (2000a). A dynamical system for neighborhoods in plant communities. *Ecology* **81**, 2137–2148.
- LAW, R. & DIECKMANN, U. (2000b). Moment approximations of individual-based models. In: *The Geometry of Ecological Interactions: Simplifying Spatial Complexity* (Dieckmann, U., Law, R. & Metz, J. A. J., eds), pp. 252–270. Cambridge: Cambridge University Press.
- LAW, R., DIECKMANN, U. & METZ, J. A. J. (2000). Introduction. In: *The Geometry of Ecological Interactions: Simplifying Spatial Complexity* (Dieckmann, U., Law, R. & Metz, J. A. J., eds), pp. 1–6. Cambridge: Cambridge University Press.
- LEVIN, S. A. & DURRETT, R. (1996). From individuals to epidemics. *Philos. Trans. R. Soc. London Ser. B-Biol. Sci.* **351**, 1615–1621.
- MATSUDA, H., OGITA, N., SASAKI, A. & SATO, K. (1992). Statistical-mechanics of population—the lattice Lotka–Volterra model. *Prog. Theor. Phys.* **88**, 1035–1049.
- MOLLISON, D. (1997). Spatial contact models for ecological and epidemic spread. *J. Roy. Stat. Soc. B* **39**, 283–326.
- NEUHAUSER, C. (1998). Habitat destruction and competitive coexistence in spatially explicit models with local interactions. *J. theor. Biol.* **193**, 445–463.
- RAND, D. (1999). Correlation equations and pair approximations for spatial ecologies. In: *Advanced Ecological Theory: Principles and Applications* (McGlade, J., ed.), pp. 100–142. Oxford: Blackwell Science.
- RHODES, C. J. & ANDERSON, R. M. (1996). Persistence and dynamics in lattice models of epidemic spread. *J. theor. Biol.* **180**, 125–133.
- SATO, K., MATSUDA, H. & SASAKI, A. (1994). Pathogen invasion and host extinction in lattice structured populations. *J. Math. Biol.* **32**, 251–268.
- TILMAN, D. & KAREIVA, P., ed. (1997). *Spatial Ecology: The Role of Space in Population Dynamics and Interspecific Interactions*. Princeton: Princeton University Press.
- VAN BAALEN, M. (2000). Pair approximations for different spatial geometries. In: *The Geometry of Ecological Interactions: Simplifying Spatial Complexity* (Dieckmann, U., Law, R. & Metz, J. A. J., eds), pp. 359–387. Cambridge: Cambridge University Press.
- WISSEL, C. (2000). Grid-based models as tools for ecological research. In: *The Geometry of Ecological Interactions: Simplifying Spatial Complexity* (Dieckmann, U., Law, R. & Metz, J. A. J., eds), pp. 94–115. Cambridge: Cambridge University Press.

APPENDIX A

Large Neighborhood Expansions for the Lattice Logistic Model

The first-order expansion for the steady-state solutions to eqn (17) is obtained by first solving eqn (17) for $\tilde{\rho}_{11}$ in terms of the other variables. Substituting this into eqn (17b,c) gives a pair of nonlinear equations for ρ_1 and ρ_{11} , and the leading order terms in ε_n , ε_f then follow from the Implicit Function Theorem:

$$\begin{aligned} \bar{\rho}_1 &\doteq \\ \bar{\rho}_1(0) &+ \frac{(b_n + d_n)(1 + d)(b_f d_n - d_n - b_n - b_n d_f)}{b(b + d)^3} \varepsilon_n \\ &+ \frac{(b - 1)(b_f + d_f)(b_f(1 - b) + d_f(1 + d))}{b(b + d)^3} \varepsilon_f, \end{aligned} \quad (\text{A.1})$$

where $\bar{\rho}_1(0)$ is the mean-field steady-state density $(b - 1)/(b + d)$. In the case of widespread offspring dispersal and localized competition we have $d_f = 0$ by eqn (21) and hence $d_n = d$. Moreover, with the total birth rate b held fixed eqn (21) implies that $b_n = O(z_n/z_f) = O(\varepsilon_f/\varepsilon_n)$ and therefore $b_f = b - O(\varepsilon_f/\varepsilon_n)$. Then dropping terms of $O(\varepsilon_f)$ from (A.1) we have

$$\bar{\rho}_1 \doteq \bar{\rho}_1(0) + \frac{d^2(b - 1)(1 + d)}{b(b + d)^3} \varepsilon_n, \quad (\text{A.2})$$

which rearranges to eqn (23); recall $\varepsilon_n = 1/\tilde{z}$ in this case. Similarly, if offspring dispersal is localized but there is long-range competition [case (20)], we have $b_f = 0$, $b_n = b$ and $d_n = O(\varepsilon_f/\varepsilon_n)$, $d_f = d - O(\varepsilon_f/\varepsilon_n)$. Substituting these into eqn (A.1), dropping $O(\varepsilon_f)$ terms, and recalling that $\varepsilon_n = 1/z$ in this case gives eqn (25). In case (22) we have $b_f = d_f = 0$, $b_n = b$, $d_n = d$ and $\varepsilon_n = 1/z$, which gives eqn (24).